

# GRID DISTURBANCE REJECTION VIA IMPROVED DC-LINK VOLTAGE FEEDFORWARD CONTROL FOR L-BEND POWER SUPPLIES IN THE APS UPGRADE\*

Y. Ruan<sup>†</sup> and F. Rafael

Argonne National Laboratory, Lemont, IL, USA

## Abstract

As part of the Advanced Photon Source Upgrade, two high-power DC supplies for the L-Bend M1 and M2 magnets were installed. During the APS-U commissioning, a 1-Hz ripple was detected in the output currents of the M1/M2 and slow corrector supplies, leading to 1-Hz beam motion. This low-frequency harmonic originated from the booster ramping supply operating at 1 Hz, causing periodic grid voltage sags. This paper proposes an improved DC-Link voltage feedforward control for the M1/M2 supplies to reject grid disturbances, significantly attenuating the 1-Hz and other low-frequency ripples in the output currents. Combined with regulation circuit modification of the slow corrector power supplies, the 1-Hz harmonic was successfully eliminated from the beam motion.

## INTRODUCTION

There are over 1,000 new bipolar power supplies for corrector magnets, along with two high-power DC supplies for the L-Bend M1 and M2 magnets, installed as part of the Advanced Photon Source Upgrade (APS-U). During the APS-U commissioning in early 2024, a 1-Hz beam motion was observed, and the booster ramping supply was identified as the source of the harmonic disturbance. Operating at 1 Hz, the ramping supply draws a significant amount of power from the 480-VAC grid, causing periodic voltage sags, as illustrated in Fig. 1. This grid disturbance introduces harmonics into the DC-Link voltage, affecting the output currents of both the M1/M2 and corrector supplies.

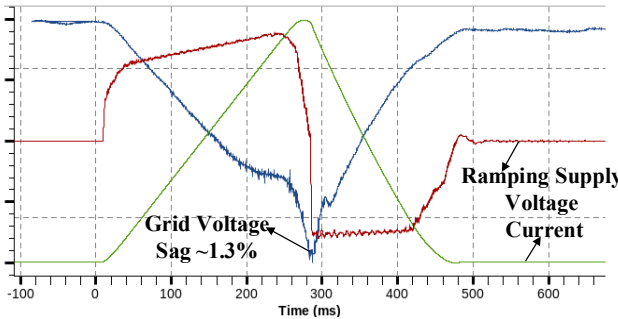


Figure 1: The voltage sag in the AC grid caused by booster ramping supply.

The corrector supplies were designed at Argonne [1-2], and the 1-Hz ripple was successfully attenuated by adjusting the regulation loop through a simple jumper

reconfiguration. However, the high-power M1/M2 supplies were designed and fabricated by a vendor, making it more challenging for Argonne to devise a solution. With limited information available, a simulation model was developed in MATLAB/Simulink to explore methods for mitigating the 1-Hz ripple. Simulation results confirmed that employing DC-Link voltage feedforward to automatically adjust the PWM duty ratio was highly effective in rejecting grid disturbances.

It was later discovered that the existing DC-Link voltage sensing circuit excluded low-frequency components, which explains why the previous feedforward control had little effect on rejecting disturbances—this finding was also confirmed by the simulation results. As a result, the DC-Link voltage sensing circuit was modified to incorporate low-frequency signals. Additionally, the controller firmware was updated to accommodate this hardware change. With the modified feedforward control in place, the low-frequency ripples, including the 1-Hz disturbance, were significantly attenuated, resulting in the successful elimination of the 1-Hz beam motion.

## GRID DISTURBANCE REJECTION FOR M1/M2 SUPPLIES

### Power Circuit and Control Scheme

The L-Bend M1/M2 supplies share a similar power circuit and control scheme, as shown in Fig. 2, with differences in power capacity. The M1 supply is rated at 475 A/1500 V DC, while the M2 supply is rated at 220 A/1000 V DC. Both supplies use an internal step-up transformer that feeds two 6-pulse rectifiers, followed by an IGBT-based bridge. The output current is regulated to track the setpoint provided by the Experimental Physics and Industrial Control System (EPICS).

For both M1 and M2 supplies, there is an outer current control loop and an inner voltage control loop, both implemented digitally in the firmware. The output of the current loop serves as the reference signal  $u_r$  for the voltage loop, and the duty ratio  $e$  is generated to regulate the output voltage  $u_{out}$ , ensuring that the output current tracks the setpoint.

### Duty Ratio Correction With DC-Link Voltage Feedforward

The DC-Link voltage feedforward (FF) is already applied in the firmware, which corrects the duty cycle  $e$  to compensate for voltage fluctuations and maintain stable output:

$$e \frac{\bar{u}_{dc}}{u_{dc}},$$

where  $\bar{u}_{dc}$  stands for the DC component of the DC-Link voltage  $u_{dc}$ . If  $u_{dc}$  fluctuates, the duty cycle is automatically corrected before the ripple from  $u_{dc}$  impacts the output current. This approach is significantly faster and more efficient than the dual-loop feedback control in attenuating the ripple coming from the DC-Link, as demonstrated in the following simulation results.

However, it was later discovered that the low-frequency ripple is filtered out by the DC-Link voltage sensing circuit, which prevents the automatic correction of the duty cycle from responding to low-frequency disturbances such as the 1-Hz ripple. The DC-Link voltage sensing circuit measures DC and AC signals separately to enhance the ADC resolution. The DC sensing circuit employs a low-pass filter with a corner frequency of 0.15 Hz, while the AC sensing circuit utilizes a high-pass filter (HPF) with a corner frequency of 4.2 Hz. Consequently, the  $u_{dc}$  measured by this method does not capture low-frequency fluctuations. As a result, the correction factor excludes these lower-frequency ripples, allowing transient ripples from grid disturbance to still appear in the output current.

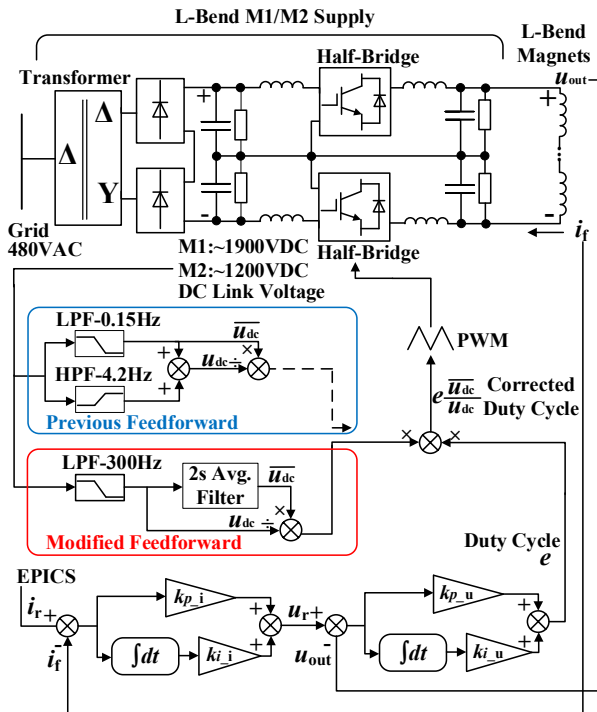


Figure 2: L-Bend power supply with improved DC-link voltage feedforward to mitigate grid disturbance.

For the M1/M2 supplies, hardware and firmware could be modified to enhance the performance of the DC-Link voltage feedforward control. The AC sensing circuit of the DC-Link voltage could be disregarded by the control firmware. By increasing the corner frequency of the DC sensing circuit from 0.15 Hz to 300 Hz, the  $u_{dc}$  measurement can capture lower frequency ripples while effectively attenuating the IGBT switching noise at the same time. The DC component  $\bar{u}_{dc}$  is calculated using a 2-second window average filter applied to  $u_{dc}$ .

A simulation model was developed using MATLAB/Simulink, and the simulation was conducted under three scenarios: without DC-Link voltage feedforward control, with the previous feedforward control, and with the modified feedforward control. The DC-Link voltage exhibited low-frequency transients, as shown in Fig. 3. When the feedforward control was absent, the peak-to-peak ripple in the current reached 228 mA. The measured  $u_{dc}$  using the previous method was significantly inaccurate, resulting in only a marginal improvement to the peak-to-peak ripple (208 mA) with the previous feedforward control. However, with the modified  $\bar{u}_{dc}$  measurement, the feedforward control substantially reduced the peak-to-peak current ripple to just 2.8 mA, representing a reduction factor of 75.

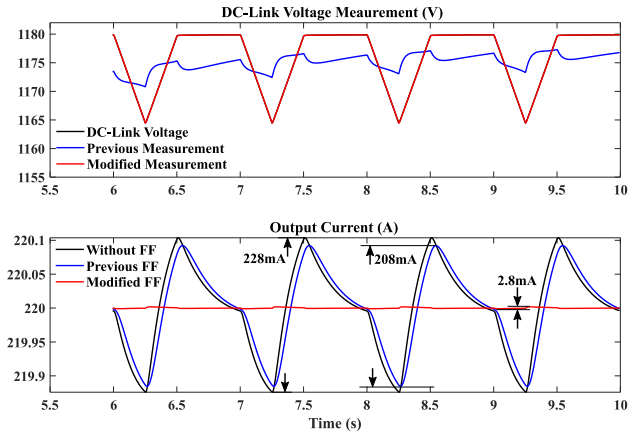


Figure 3: Simulation results of DC-link voltage feedforward on L-Bend M2 supply.

## OPERATIONAL RESULTS

### L-Bend Supply

Both hardware and firmware modifications, as described in the previous section, were implemented for M1 and M2 supplies to enhance the performance of the DC-Link voltage feedforward control. The ripple current for the L-Bend M1 supply was measured using both the previous DC-Link voltage feedforward and the modified feedforward control.

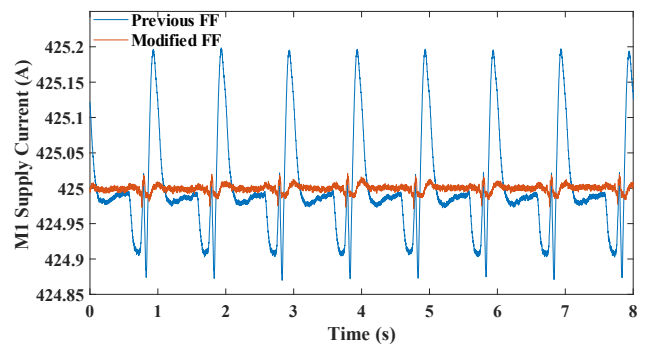


Figure 4: M1 current waveform.

Figure 4 displays the current waveforms, demonstrating a noticeable reduction in peak-to-peak ripple with the improved feedforward control. Figure 5 presents the ripple

spectrum, highlighting that the lower-frequency ripple values from 1 Hz to 10 Hz are significantly lower than those obtained with the previous feedforward method. Figure 6 shows the exact ripple values (mA RMS), clearly indicating that the modified feedforward control greatly attenuates the low-frequency ripples in M1 introduced by periodic grid sag. For instance, the 1-Hz, 2-Hz, and 3-Hz ripples are reduced by factors of 44.3, 24.1, and 11.6, respectively, decreasing from 30.10 mA, 34.64 mA, and 16.7 mA to 0.68 mA, 1.44 mA, and 1.14 mA. A similar improvement is also observed in the M2 supply.

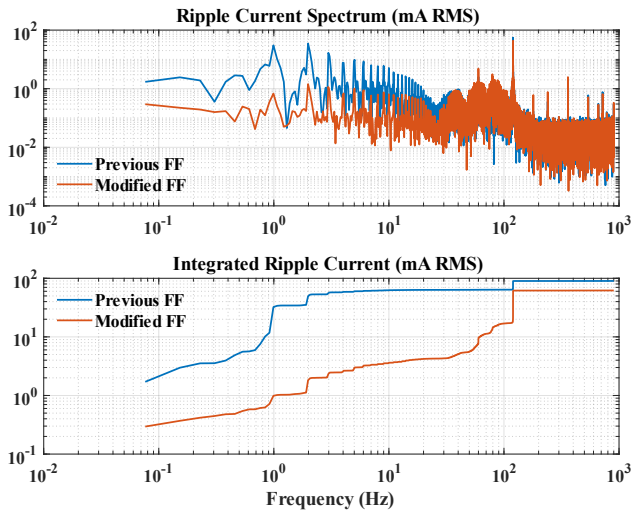


Figure 5: Ripple current spectrum of L-Bend M1 supply at 425 A.

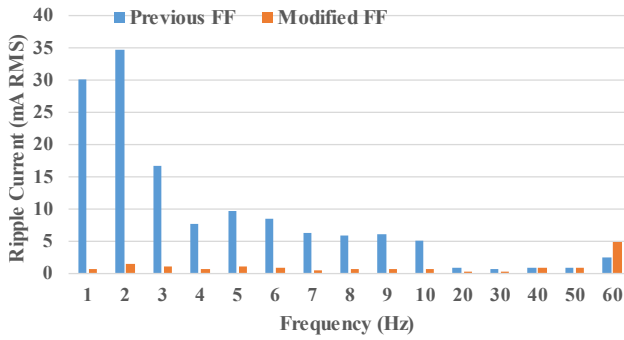


Figure 6: M1 Ripple currents (mA RMS) among 1 Hz and 60 Hz.

### Beam Motion Improvement

The slow corrector power supplies were tuned at the same time to mitigate the grid disturbance via a simple jumper-reconfiguration that accelerated the regulation response. Figures 7 and 8 present the median integrated beam motion from all P0 beam position monitors before and after tuning of corrector and M1/M2 supplies. It clearly indicates that the sharp increases at 1 Hz, 2 Hz, and 3 Hz have been eliminated, which corresponds to the significant attenuation of low-frequency current ripples from those supplies. However, the beam motion still exhibits 30-Hz and 60-Hz ripples, the source of which are currently under investigation.

## CONCLUSION

This paper presented a method to address the 1-Hz transient ripple caused by grid disturbance for the L-Bend magnet power supplies in the APS Upgrade. The control firmware and hardware were modified to enhance the DC-Link voltage feedforward control, specifically by incorporating the low-frequency signals in feedforward. This approach successfully rejected periodic grid disturbances and removed the 1-Hz transient from the output currents. In combination with the slow corrector supplies tuning, the 1-Hz beam motion has been effectively eliminated.

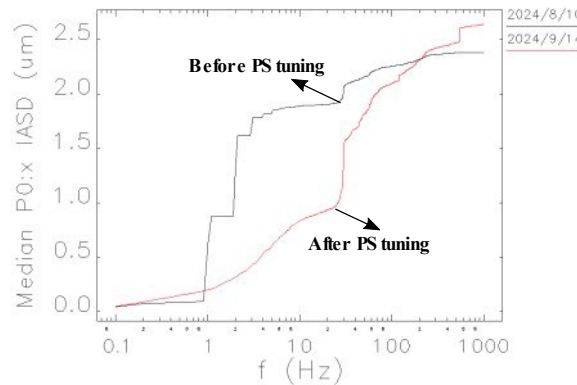


Figure 7: Median integrated beam motion of P0 at x panel.

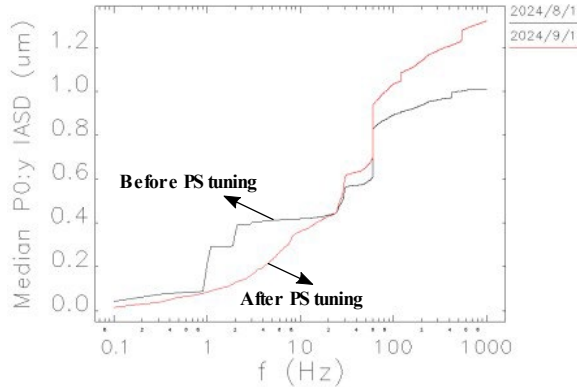


Figure 8: Median integrated beam motion of P0 at y panel.

## REFERENCES

- [1] J. Wang and G. S. Sprau, "A High Bandwidth Bipolar Power Supply for the Fast Correctors in the APS Upgrade", in *Proc. NAPAC'16*, Chicago, IL, USA, Oct. 2016, pp. 96-98. doi:10.18429/JACoW-NAPAC2016-MOPOB12
- [2] J. Wang, I. A. Abid, R. T. Keane, and G. S. Sprau, "Preliminary Designs and Test Results of Bipolar Power Supplies for APS Upgrade Storage Ring", in *Proc. IPAC'18*, Vancouver, Canada, Apr.-May 2018, pp. 2381-2383. doi:10.18429/JACoW-IPAC2018-WEPMF008